Materials Physics and Mechanics. 2022;48(3): 397-406
Research article
http://dx.doi.org/10.18149/MPM.4832022_10

Submitted: March 23, 2021
Approved: May 16, 2022
Accepted: June 6, 2022

Study numerical and experimental of stress concentration factor on isotropic plate with hole

M.N. Misbah✉, R.C. Ariesta, T. Yulianto, D. Setyawan, W.H.A. Putra

Sepuluh Nopember Institute of Technology, Jalan Raya Kampus ITS Sukolilo, Surabaya 60111, Indonesia

✉ mnmisbah@na.its.ac.id

Abstract. The stress concentration factor (SCF) can lead to the failure of ship construction. That problem can occur with hotspot stress expansion in the local area because of the acting load and structural details shapes. However, there is no method for the asses of structure design failure in the minor openings such as a dry hole and scallop dimension. Furthermore, the research aims for evaluating stress concentration performed using the diameter and width (d/W) ratio. The model of plates generates to identify stress phenomena on the isotropic ship plate. The numerical simulation was carried out using finite element analysis and proven by experimental method with the installation of the strain measurement on several working loads of 30% and 60% under yield strength. The plate used for analysis is an A36 steel plate commonly used in the shipbuilding industry. The plate model with the hole was identified, which shows the stress concentration that occurs increases after the d/W of the isotropic plate also increases, then the comparative stress plot. Moreover, based on the numerical and experimental analysis, the comparisons of stress concentration factors within different radius holes have been completed for assessment. Finally, result from numerical and experimental obtained error values below 3%.

Keywords: stress concentration factor, ship, numerical, experimental

Acknowledgements*. The work is supported by Beginners research funding fund from Research Institution Institut Teknologi Sepuluh Nopember, Surabaya. We thank our colleagues from Ship Strength and Construction Laboratory, who provided insight and expertise that greatly assisted the research, although they may not agree with all of the interpretations/conclusions of this paper.*

Citation: Misbah MNM, Ariesta RCA, Yulianto TY, Setyawan DS, Putra WHAP. Study numerical and experimental of stress concentration factor on isotropic plate with hole. *Materials Physics and Mechanics.* 2022;48(3): 397-406. DOI: 10.18149/MPM.4832022_10.

1. Introduction

Stress Concentration Factor (SCF) is a number that will increase when a plate gets tension force concentrated, such as holes and changes in the cross-section. Recently the sharper radius at the cross-section will influence the increasing SCF value. The plate pressure work per the dimensions of the hole diameter occurs on the plates, the number of the holes, and the axial force that works. The plate holes resulting in a pressure differential force on the other size determine the value. Application of SCF in ship structures like dry holes, corner edge containers, and scallops choose to obtain the best model for reducing stress. The methods performed to determine the SCF model on the plate have several steps. First steps

experiments [1,2], numerical model, regression analysis, finite element [3,4], and artificial intelligence (AI). Numerical model using finite element analysis package software and verifying used experiment tensile test using a universal tensile machine (UTM). To become a numerical example stress intensity factor in evaluating a two-dimensional crack [5,6] is the Stress concentration factor obtained from the plate in a flexible environment. The maximum stress and stress concentration factors appear inconstantly occur at the hole [1]. Reducing SCF is also determined by selecting the appropriate shape. The sharpness of form can construct the concentration of high-stress concentration. Material with a large SCF will quickly fail [2]. This research aims to obtain the result of the stress concentration on the plate material on the vessel. For example, several holes found on the ship structure are all-important, such as lightning holes, which also lead to detection of stress concentration and need analysis to prevent damage on construction with an additional hole or change to optimum shape [3]. This research observed how many errors in the numerical and experimental. Therefore, analysis of the deviation that appears.

2. Research Purposes

Stress occurs when the body gets an external force. Especially that happens on the ship hull as a critical area, and to prevent that, external and internal forces will reduce by applying holes to direct a working load focus on the one spot. To predict that stress only appears when to the part and given the treatment so that the structure has good resistance to loading. The research has specific aims:

a. Obtain the stress concentration factor on a plate with a hole with a various nation of diameter using experimental and numerical
b. Determine a Comparison of stress testing the value of concentration factor with experimental and numerical verification.

3. Research Methods

Tensile Test. Tensile testing on the A36 material was carried out to determine the amount of force needed by the material to exceed the yield strength limit to material forces in plastic conditions as input of modelling. The other purpose tensile test is to verify that the material is A36. Furthermore, check the test results in Table 1 and Table 2. Moreover, the material before and after the test is shown in Fig. 1.

Based on the tensile test, the force on the material yield was 44.67 KN, so a various loading model variance was used, with a 30% yield of 13.4 KN and a 60% yield of 26.8 KN, and a 90% yield of 40.2 KN.

Table 1. Material A36 Tensile Test Result (1/2)

Report on Test								
ASTM A36								
No	Material Code	Specification Sample			Tensile Test Result			
		Width	Thick	CSA	Yield Stress	Ultimate Stress	Elongation	Reduct of Area
		mm	mm	mm^2	Mpa	Mpa	%	%
1	A36	25.35	6	152.1	282.71	335.31	37.94	72.93
2		25.3	6	151.8	296.44	335.97	37.77	72.62
3		25.15	6	150.9	304.84	337.97	32.99	77.87

Table 2. Material A36 Tensile Test Result (2/2)

No	F.Yield (KN)	F.ultimate (KN)	Lo	L1	Wd1	Th1	A1
1	43	51	69.68	96.12	17.3	2.38	41.17
2	45	51	64.86	89.36	16.69	2.49	41.56
3	46	51	69.41	92.31	17.04	1.96	33.4

Fig. 1. Tensile Test Specimens A36

Experimental Model. The material verification approved the validity by ensuring that it adhered to the issue boundaries mentioned earlier, resulting in a conclusion in good agreement with the facts at the end of the experiment's review [10,11]. Supplying the critical material, A36 steel, and working equipment like a drill, hacksaw, solder, sandpaper, ruler, glue, and tape, are all part of the material preparation process. The specimen dimensions have a length of 300 mm, a width of 60 mm, and a thickness of 6 mm. The test material hole diameter varies between 6 mm, 18 mm, and 30 mm, as shown in Figs. 2-4.

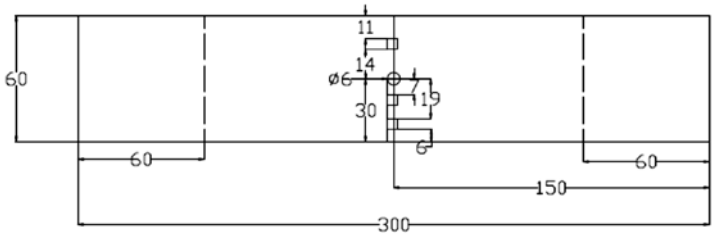

Fig. 2. Test Material Design 1

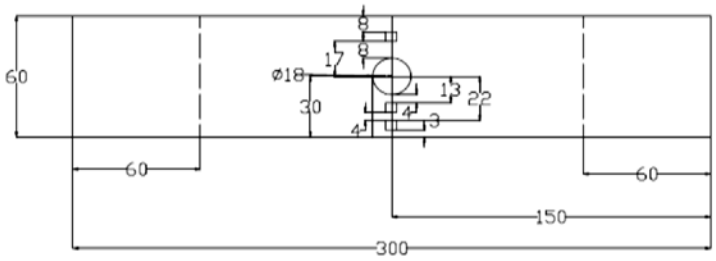

Fig. 3. Test Material Design 2

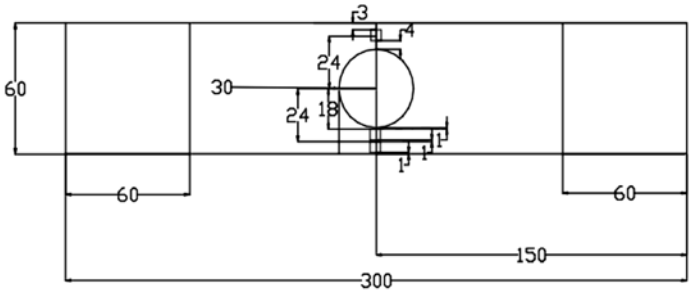

Fig. 4. Test Material Design 3

The sensor used in the experiment is a strain gauge with 350 ohms. Before installing the sensor, polish the surfaces of the steel specimen with sandpaper of grades 150-1200 to achieve a glossy finish and clean with alcohol. The adhesive function joins the sensor with the surface material and the tape patch on it as an additional method to minimize hand contact. There were four sensors installed: one for normal stress distribution and three for stress conversion sensors. The material was tested by tensile testing with three different load variants, as shown in Fig. 5, i.e. 30% yield (13,400 N), 60% yield (26,800 N), and 90% yield (40,200 N). An arrangement of sensor settings with the channel position. The first was at the nearest hole, the second was in the among sensor, the third was on the edge material, and the sensor recorded forces in the Y-axis direction.

Fig. 5. Measurement process setup

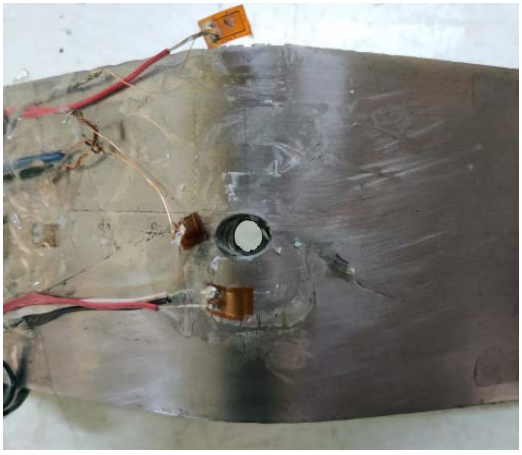

Fig. 6. Broken specimen

The sensor will detach after the force enters the plastic zone. Furthermore, measuring the load used to calculate the stress concentration obtained, a broken specimen will be illustrated in Fig. 6.

Numerical Model. Steel was chosen as a material commonly used in ship construction. The dimension of a plate with a size of 300 mm × 60 mm × 6 mm was modelled by three different variations of the diameter of the holes, specifically, 6 mm, 18 mm, and 30 mm. The material properties defined such as Young's modulus (*E*), density (ρ), and Poisson's ratio (υ) were presented in Table 3.

Table 3. Material properties of steel plate

Material	*E* (MPa)	ρ (kg/m^3)	υ
Steel	210×10^6	7850	0.26

The numerical simulation will investigate using finite element software ABAQUS^{TM}. Eight-node solid linear brick element (C3D8R) implement into the specimen model. Moreover, Steel defines as a homogenous specimen. The boundary condition applied on the top surface was assumed to be clamped on the grip of UTM. Therefore, the load is applied to the bottom of the surface area as a tensile test.

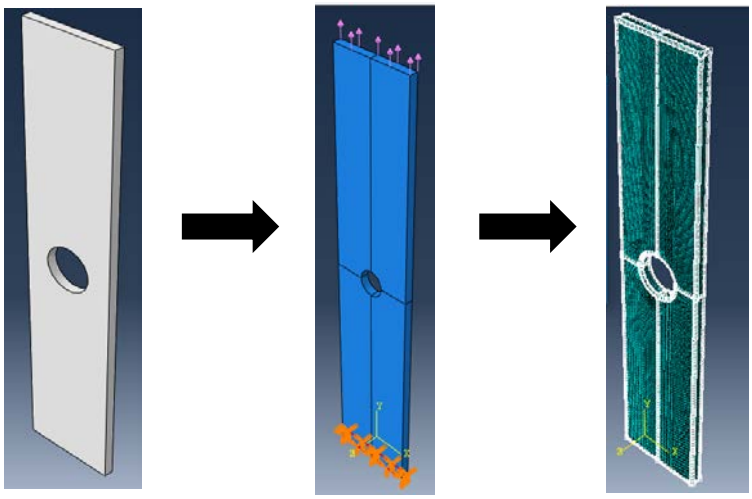

Fig. 6. Specimen model discretization

A Discretization stages cover mesh convergence that aims to ensure the stability of numerical analysis. According to theory, detailed size elements of results will increase the accuracy of the simulation [4]. The results data obtained from the simulation are several stress components such as von Mises stress, Y-axis stress, and X-direction stress. These results use to calculate the stress concentration factor, with the Y-axis stress in the same direction as the tensile test force of each model. When the created model is appropriate, verification was required by performing meshing optimization in software or convergence to obtain a constant stress value at the optimal meshing for further analysis [5]. The final stress is divided into some types of stress obtained from a statistical equation to produce the SCF, stress concentration factors at load variations of 30%, 60%, and 90% of yield strength load.

4. Result and Discussion

Data were read from a strain gauge sensor and attached to the P3 micro Measurement Model to obtain the strain in micro-strain units (106), multiplied by the Modulus of Material (E) generating the stress. The test results are shown in Table 4.

Table 4. Tensile Test Result for Experimental Method

d (mm)	Strain 30%	Strain 60%	σNom (MPa)		Strain 30%	Strain 60%	σMax (MPa)	
6	0.000194	0.000381	40.7	80.10	0.000512	0.001015	107.9	213.2
18	0.000240	0.000496	50.5	104.1	0.000561	0.001159	117.9	243.4
30	0.000350	0.000689	73.4	142.5	0.000753	0.001464	158.1	307.4

The stress concentration factor is obtained by calculating the maximum stress ratio compared to the nominal stress so that the SCF is obtained on the test material using the strain gauge sensor with the results in Table 5.

Table 5. Stress Concentration Factor of Tensile Test Experimental Method

σ_{nom} (MPa)		σ_{max} (MPa)		SCF 30%	SCF 60%
Strain 30%	Strain 60%	Strain 30%	Strain 60%		
40.9	80.10	107.95	213.21	2.64	2.66
50.58	104.14	117.90	243.48	2.33	2.34
73.43	142.56	158.14	307.44	2.15	2.15

The maximum stress data obtained was used to calculate the amount of SCF based on different variations of the hole size. The stress concentration factor (SCF) is a dimensionless factor used to measure stress concentration [6]. The SCF value determines by calculating using Eq (1):

$$\text{SCF} = \frac{\sigma_{max}}{\sigma_{nom}}. \quad (1)$$

It means the ratio of the maximum stress to nominal stress. The nominal stress is total stress in an element under the same loading conditions without a stress concentration to calculate the perforated acting load on the plate [6] Eq.(2):

$$\sigma_{nom} = \frac{P}{(W-d)\times t}, \quad (2)$$

where load (P), a width of material (W), hole diameter (d), and thickness of plate (t). Moreover, the SCF results from empirical calculations can be seen in Tables 6-8 using various loads of 30%, 60%, and 90% yield force.

Table 6. Tensile Stress Y-Axis, load 30% yield

Model	d/w	w=60mm	t=6mm		SCF
		Hole size (d) (mm)	Load (30% yield=13.4 KN)		
			Maximum Stress (MPa)	Nominal Stress (MPa)	
1	0.05	3	105.79	39.18	2.70
2	0.1	6	107.49	41.36	2.60
3	0.3	18	123.24	53.17	2.32
4	0.5	30	159.42	74.44	2.14

Table 7. Tensile Stress Y-Axis, load 60% yield

Model	d/w	w=60mm	t=6mm		SCF
		Hole size (d) (mm)	Load (60% yield=26.8 KN)		
			Maximum Stress (MPa)	Nominal Stress (MPa)	
1	0.05	3	211.58	78.36	2.70
2	0.1	6	214.98	82.72	2.60
3	0.3	18	246.48	106.35	2.32
4	0.5	30	318.83	148.89	2.14

Table 8. Tensile Stress Y-Axis, load 90% yield

Model	d/w	w=60mm	t=6mm		SCF
		Hole size (d) (mm)	Load (90% yield=40.2 KN)		
			Maximum Stress (MPa)	Nominal Stress (MPa)	
1	0.05	3	317.37	117.54	2.70
2	0.1	6	322.50	124.07	2.60
3	0.3	18	369.76	159.52	2.32
4	0.5	30	478.29	223.33	2.14

Calculation of the Stress Concentration Factor using the Empirical Method. The empirical calculation method determines using Eq.(3) after obtaining the SCF value based on the FEA simulation test results for each test model selecting Y direction stress for collecting the nominal data is summarised in Table 9 [12].

$$SCF = 3.00 = 3.13\left(\frac{2r}{D}\right) + 3.66\left(\frac{2r}{D}\right)^2 - 1.53\left(\frac{2r}{D}\right)^3. \quad (3)$$

Table 9. SCF Calculation for Empiris Tensile (Roarks Formula)

Variation	r (mm)	W (mm)	d/w	SCF
Model 1	1.5	60	0.05	2.85
Model 2	3		0.1	2.72
Model 3	9		0.3	2.35
Model 4	15		0.5	2.16

Comparison of the SCF using different methods. From the Roarks, numerical and experimental results were compared to evaluate that error [12]. All the results of the SCF calculations for each test model are summarised in Table 10.

The stress concentration factor is sensitive to the ratio, and the experiment shows that the higher the ratio value, the higher the maximum stress, and the smaller the SCF value. The average of SCF with various loadings is explained in Table 11.

The graph shows in Fig. 7 a similar trend and pattern, which means the method to evaluate stress concentration factor (SCF) can perform. The value of SCF at 0.1 d/w around 2.7-2.8, in d/w 0.3 that narrow to 2.4, and at d/w is 0.5 that value very close to about 2.2.

Table 10. Comparison of SCF Calculations

d (mm)	(d/W)	Numerical			Experimental		SCF (Roarks Formula)	Empirical Numeric Difference (%)	Numerical Experiments Difference (%)
		30%	60%	90%	30%	60%			
		SCF	SCF	SCF	SCF		SCF		
3	0.05	2.70	2.70	2.70			2.85	5.26	
6	0.1	2.60	2.60	2.60	2.64	2.66	2.72	4.45	1.94
18	0.3	2.32	2.32	2.32	2.33	2.34	2.35	1.38	0.71
30	0.5	2.14	2.14	2.14	2.15	2.15	2.16	0.86	0.62

Table 11. Average of SCF for Tensile Test

Hole Diameter Lingkaran (d) (mm)	W (60 mm)	Numerical Method	Experimental Method	Roarks Formula
	d/W	SCF		
3	0.05	2.70	-	2.85
6	0.1	2.60	2.65	2.72
18	0.3	2.32	2.33	2.35
30	0.5	2.14	2.15	2.16

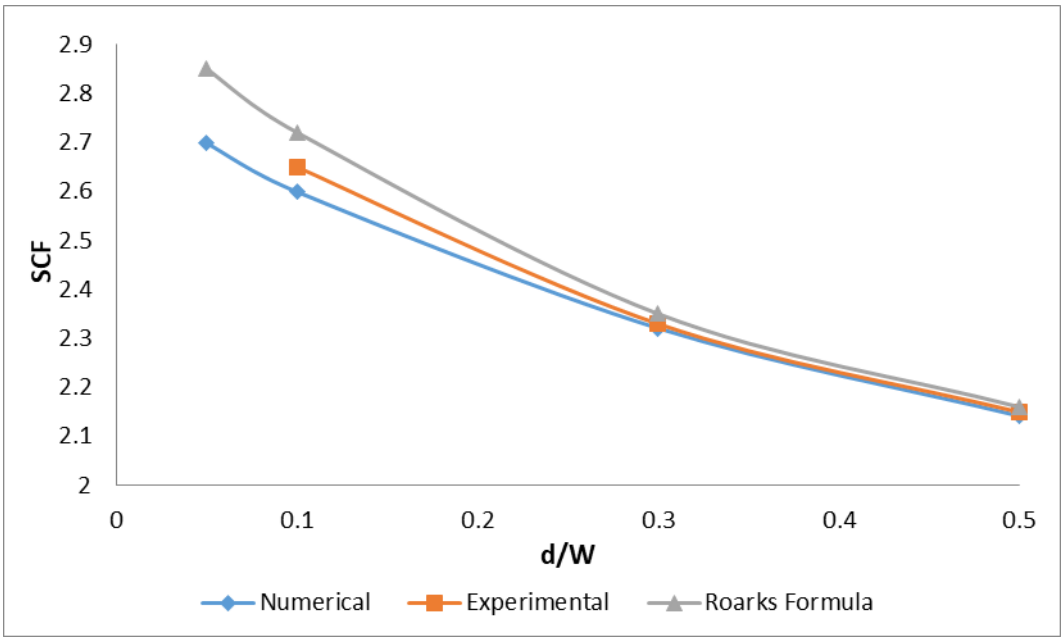

Fig.7. Average of SCF for Tensile Test

5. Conclusions

The Experimental (Strain Gauge Sensor) and Numerical (Finite Element Method) measurement methods are used in this study to determine the value of the Stress Concentration Factor (SCF) value, and the results are compared to draw the following conclusions:

1. The numerical method stress concentration factor with a load of 30%, 60%, and 90% did not change at 6 mm, 18 mm, and 30 mm diameters with 2.60, 2.32, and 2.14, respectively. While the experimental method, loading 30%, 60% experienced a change in

6mm diameter from 2.64 (30% load) to 2.66 (60% load), 18mm diameter from 2.33 (30% load) to 2.34 (60% load), 30mm diameter not change remains at the value 2.15.

2. The SCF value calculated using experimental and numerical methods is in good agreement, with a difference of less than 3%.

References

1. Sarangi H, Murthy K, Chakraborty D. Experimental verification of optimal strain gage locationsfor the accurate determination of mode I stress intensity factors. *Engineering Fracture Mechanics.* 2013;110: 189-200.

2. Suardana N, Sugita I, Wardana I. Hybrid Acoustic Panel: The Effect of Fiber Volume Fraction and Panel Thickness. *Material Physics and Mechanics*. 2020;44(1): 77-82.

3. Takaki Y, Gotoh K. Approximate weight functions of stress intensity factor for a wide range shapes of surface and an embedded elliptical crack. *Marine Structures.* 2020;70: 1-22.

4. Sujiatanti SH, Yulianto T, Putra WHA, Ariesta RC. Influence of the Cut-out Shape on the Fatigue Ship Structural Detail. In: *Proc. of 6th International Seminar on Ocean and Coastal Engineering, Environmental and Natural Disaster Management*. 2018. p.111-115.

5. Tanaka S, Okada H, Okazawa S, Fujikubo M. Fracture mechanics analysis using the wavelet Galerkin method and extended finite element method. *International Journal for Numerical Methods in Engineering.* 2013;93(10): 1082-1108.

6. Sujiatanti SH, Tanaka S, Shinkawa S, Setoyama T, Yanagihara D. Experimental and numerical studies for buckling and collapse behaviors of a cracked thin steel panel subjected to sequential tensile and compressive loading. *Thin-Walled Structures.* 2020;157: 1-14.

7. Yang CZ, Cho C, Kim HB, Beom G, The effect of biaxial load on stress and strain concentrations in a finite thickness elastic plate containing a circular hole. *International Journal for Numerical Methods in Engineering.* 2008;75(1): 103-126.

8. Sumi Y, Yajima H, Toyosada, Masahiro, Yoshikawa T, Aihara S, Gotoh K, Ogawa Y, Matsumoto T, Hirota K, Hirasawa H, Toyoda M, Morikage Y. Fracture control of extremely thick welded steel plates applied to the deck structure of large container ships. *Journal of Marine Science and Technology.* 2013;18: 497-514.

9. Ariesta RC, Zubaydi A, Ismail A, Tuswan T. Damage evaluation of sandwich material on side plate hull using experimental modal analysis. *Materials Today: Proceedings*. 2021;47: 2310-2314.

10. Ariesta RC, Zubaydi A, Ismail A, Tuswan T, Identification of Damage Size Effect of Natural Frequency on Sandwich Material using Free Vibration Analysis. *Naše More.* 2022;69(1): 1-8.

11. Putri R, Yulianto T, Ariesta RC, Misbah MN. Influence of Stress Concentration Factor due to Scallop Form on the Wrang Plate Structure. *Kapal: Jurnal Ilmu Pengetahuan dan Teknologi Kelautan.* 2022;19(1): 29-41.

12. Misbah MN, Sujiatanti SH, Setyawan D, Ariesta RC and Rahmadianto S. Structural Analysis on the Block Lifting in Shipbuilding Construction Process. *MATECT Web of Conferences.* 2018;177: 01027.

13. Young WC, Budynas RG. *Roark's Formula for Stress and Strain.* New York: McGraw-Hil; 2002.

THE AUTHORS

Misbah M.N.
e-mail: mnmisbah@na.its.ac.id
ORCID: -

Ariesta R.C.
e-mail: chandra14@mhs.na.its.ac.id
ORCID: 0000-0002-5510-6369

Yulianto T.
e-mail: totoky@na.its.ac.id
ORCID: -

Setyawan D.
e-mail: dony@na.its.ac.id
ORCID: 0000-0003-2498-051X

Putra W.H.A.
e-mail: wing@na.its.ac.id
ORCID: -